Proceedings of ASME Turbo Expo 2010: Power for Land Sea and Air
GT2010
June 14-18, 2010, Glasgow, UK

GT2010-23642

INFLUENCE OF EXHAUST GAS RECIRCULATION ON COMBUSTION INSTABILITIES IN CH4 AND H2/CH4 FUEL MIXTURES

Don Ferguson
National Energy Technology Laboratory – US
DOE Morgantown, WV, USA

Joseph A. Ranalli
National Energy Technology Laboratory – US
DOE Morgantown, WV, USA

Peter Strakey
National Energy Technology Laboratory – US DOE
Morgantown, WV, USA

ABSTRACT

This paper evaluates the impact of two strategies for reducing CO2 emissions on combustion instabilities in lean-premixed combustion. Exhaust gas recirculation can be utilized to increase the concentration of CO2 in the exhaust stream improving the efficiency in the post-combustion separation plant. This coupled with the use of coal derived syngas or hydrogen augmented natural gas can further decrease CO2 levels released into the environment. However, changes in fuel composition have been shown to alter the dynamic response in lean-premixed combustion systems. In this study, a fully premixed, swirl stabilized, atmospheric burner is operated on various blends of H2/CH4 fuels with N2 and CO2 dilution to simulate EGR. Acoustic pressure and velocity, and global heat release measurements were performed at fixed adiabatic flame temperatures to evaluate the impact of fuel composition and dilution on various mechanisms that drive the instabilities.

INTRODUCTION

Growing concerns over the release of greenhouse gas emissions into the atmosphere have generated interest for reducing point source emissions of Carbon Dioxide (CO2). It is estimated that electricity generation accounts for approximately 41% of all CO2[1], and projections suggest an increase of 54.3% in electricity generation from the combustion of fossil fuels world-wide over the next 20 years[2] thus emphasizing the urgency for developing viable strategies for reducing CO2 emissions. Three basic ideologies exist for reducing CO2 emissions from combustion related to power generation: 1) improvements in overall system efficiency, 2) capturing or sequestering CO2 emissions and / or 3) increase utilization of low carbon fuel or renewable sources. As a growing percentage of power is generated by gas turbine based systems burning natural gas, it is imperative to understand how these CO2 mitigation strategies will impact combustion performance. Any of these general strategies could involve changes in fuel composition, such as utilizing coal-derived syngas, hydrogen/hydrocarbon blends, biogas or waste gas streams as fuels or incorporating exhaust gas recirculation (EGR) to maximize CO2 concentration in the exhaust.

Changes in fuel composition lead to variations in combustion phenomena such as NOx emissions, flashback, lean blow-off and/or dynamic instabilities. This study will investigate the influence of simulated (EGR) on dynamic combustion instabilities in methane and methane/hydrogen blended fuels. Tests are performed on a lab-scale, swirl stabilized, atmospheric burner. EGR is simulated by the addition of 0-10% CO2 and 0-20% N2. Perturbations in pressure, velocity and heat release are recorded along with time-averaged images of the unstable flame over a range of equivalence ratios and flow rates. Fuel compositions and operating conditions were pre-determined to ensure test cases with overlapping flame temperatures.

BACKGROUND

In systems that utilize post-combustion capture and storage, or sequestration, of carbon, CO2 can be separated from the flue gas using an amine-based[3] or solid[4] absorbent. Recent estimates suggest that adding a CCS to an existing plant could add as much as 30% to the cost of electricity[5], and operation of the separation process produces a noticeable impact on overall plant efficiency. Exhaust gas from a natural gas fired gas turbine may contain approximately 4-14% CO2, however, post-combustion CCS systems must be sized to accommodate the total exhaust flow requiring large and expensive equipment. Flue gas CO2 concentrations can be increased through the

application of exhaust gas recirculation (EGR), in which a portion of the exhaust flow is re-introduced at the inlet of the compressor. EGR has the added benefit of reducing NOx emissions by lower peak flame temperature in the combustor. El Kady et al.[6] demonstrated a 50% reduction in NOx emissions with 35% EGR. Similar results were obtained by Rokke et al.[7] and Li et al.[8]. In addition to CO2, EGR introduces other diluents such as N2 and H2O, which can have an impact on combustion in various ways aside from lower the peak flame temperatures. Lieuwen et al.[9] suggest diluents can impact the flame by altering the 1) mixture specific heat and adiabatic flame temperature, 2) chemical kinetic rates, and 3) radiative heat transfer.

Understanding the impact of fuel diluents, as well as unconventional fuels is important as low carbon and sustainable fuels make up a greater percentage of the domestic fuel supply. Domestic natural gas (NG) supplies are typically composed of greater than 90% methane with small amounts of heavier hydrocarbons (ethane and propane) and inerts such as nitrogen, carbon dioxide and water vapor[11]. Fuel sources such as landfill gas could have as much as 60% CO2 with the remainder being primarily CH4 and small amounts if N2. Chemical kinetic studies such as Cong and Dagaut[11] have shown that although the primary influence of CO2 is through a thermal effect, there is a secondary chemical effect through the reaction CO + OH = CO2 + H that results in a decrease in the rate of fuel consumption. In terms of combustion instabilities it is important to understand how changes in fuel composition will affect the convective time delay between acoustic disturbances and the flame center of mass.

Dynamic, or thermoacoustic instabilities, are the result of closed-loop coupling between system acoustics and unsteady heat release. This coupling is dependent upon the phase relationship between acoustic pressure and heat release perturbations. This phasing is governed by convective and chemical time scales which can vary depending on fuel composition. Lieuwen and Zinn[10] discussed how small changes in the fuel-air mixture could produce significant changes in the convective time delay and subsequently heat release oscillations for lean-premixed flames. Investigation by Fritsche et al.[20] found the transition from stable to unstable flames was associated with a critical flame temperature and a ratio of hydrodynamic time scale to chemical time scale, or Damkohler number (Da). Defining the chemical time scale as a function of the thermal diffusivity and flame speed and the hydrodynamic time scale as a function of the free stream velocity at the burner exit relates translation time of the disturbance to the flame and interaction time of the disturbance with the flame.

A number of other studies have considered the influence of fuel composition on combustion instabilities[9,13,14,15,16,17]. Operating on simulated syngas with CO and H2 ranging from 20-80%, Speth et al.[21] suggested that changes in the dynamic response were controlled by interactions between the flame and inner/outer recirculation zone vortices and the time scales associated with vortex shedding and chemical kinetic processes. Wicksall and Agrawal[14] investigated the influence of hydrogen augmentation on methane flames with results indicating an increase in the total sound power with an increase in the adiabatic flame temperature. A similar study performed by Tuncer et al.[22] considered the dynamic response of a hydrogen-enriched methane flame giving anecdotal evidence of a change in the flame center of mass as a result of an increase in flame speed. Unfortunately supportive quantitative results were not provided. Hendricks and Vandsburger[15] measured the Frequency Response Function of various hydrocarbon flames exposed to open-loop forcing of the flame and showed that varying the fuel content could drive or damp the instability depending on the mode of the instability. The concept of mode hopping as a result of varying the convective time delay was discussed in detailed by Richards et al.[16].

Combustion instability mechanisms such as equivalence ratio perturbation or vortex shedding originate within the premixer, injector or combustor. These disturbances are convected to the flame where they produce a perturbation in the combustion heat release which in turn drives the instability[10]. Richards et al.[16] discussed this time-delay model and argued that in order for closed-loop dynamics to occur the time delay must be a function of the acoustic period, T = 1/f where "f" is the frequency, thus $\tau = kT$ which is dependent on the acoustic characteristics of the combustion chamber. The convective time delay can be expressed as a relationship between the some convective and chemical time scale[9]:

$$\tau_{conv} + \tau_{chem} = kT \qquad (1)$$

where τ_{conv} represents the time required for a disturbance to propagate from its point of origin to the flame "center of mass", and τ_{chem} is the chemical time that elapses as a result of combustion at the flame center of mass. Both of these terms could vary with fuel composition, for example a fuel with a lower flame speed could elongate the flame pushing the center of mass further downstream while having a slower rate of fuel consumption. The remaining paper describes efforts aimed at identifying the influence of fuel dilution in the form of simulated exhaust gas recirculation on the convective time delay, and subsequently on the dynamic response of the burner.

EXPERIMENTAL FACILITIES AND PROCEDURES

The experimental apparatus used for this study is an atmospheric pressure laboratory-scale, swirl stabilized dump combustor. A schematic of the burner and diagnostics is shown in Fig. 1. The inlet nozzle is a 21.6mm dia tube with an 8.8mm centerbody. The combustion section has an open-closed configuration with a 79mm inner diameter and is 0.56 m long quartz resonator tube to allow self-excited combustion instabilities to occur. The swirler was located 38 mm upstream of the dump plane and had a geometric swirl number of 0.88. Reynolds numbers at the end of the delivery tube varied approximately over the range of 6000 to 10000 for the lowest flow and highest flow cases, respectively. Fuel, air and

diluents were metered by a series of mass flow controllers, and were well mixed prior to passing through a choke plate in the base of the combustor. This ensured that no coupling between the acoustics and the mixing could occur.

Data was initially obtained from the flame under steady conditions without the presence of self-excited instabilities. To achieve steady flame conditions the 0.56 m tube was replaced with a shorter quartz tube of approximately 0.2 m in length. This altered the acoustic characterisitics of the system and permitted stable operation of the flame at all operating conditions.

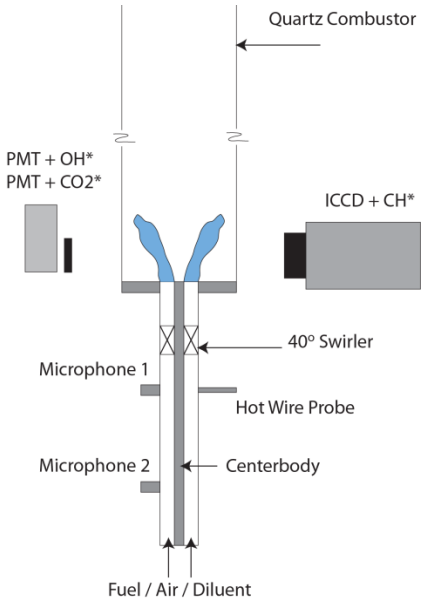

Figure 1 - Schematic diagram of the closed-end burner and experimental apparatus

A variety of diagnostics were used to characterize the oscillations. A hotwire anemometer was inserted into the flow upstream of the swirler to measure the axial acoustic velocity. The RMS value of the oscillating component of the velocity was used to represent the amplitude of instability. In addition, two photomultiplier tubes (PMTs), Hamamatsu R758 and R212UH coupled with narrow bandpass filters, were used to independently detect the OH* (308 nm) and CO2* (365 nm) chemiluminescence signals, respectively. Light was directed onto each PMT through a focusing lens in order to image the entire flame. These chemiluminescence emitters are known to be indicators of the flame heat release rate[18]. However, chemiluminescence radiation intensity is known to have a nonlinear dependence on flame temperature[19]. As such, chemiluminescence is used in this study as a phase reference for the heat release, while absolute intensity of the heat release rate was not evaluated.

In addition to global chemiluminescence, spatially resolved chemiluminescence was recorded using an intensified camera narrow band filtered at 431 nm for CH* emission. These images were acquired with an intensifier gate of 5ms, approximately integrating over one full cycle of the unstable operation (around 200Hz). Ten such images were averaged at each operating condition to reduce the impact of transient behavior, Fig 2a. Each average image was deconvoluted assuming axial symmetry using an Abel Transform (Fig 2b), and the axial (from the dump plane), and radial (from the centerline) offset distance to the flame center-of-mass were calculated for each image.

Table 1 – Operating Map for the experiments. Diluent composition is a percentage of the total flow. Fuel composition is reported as a percentage of the fuel flow only.

	A	B	C	D	E	F
Phi	0.65-1.10	080-1.10	0.75-1.10	0.85-1.10	0.80-1.10	0.75-1.10
Total Flow (LPM)	100-150	100-150	100-125	100-150	100-150	100-140
Diluent Comp.						
CO2 (% Total)	0	10	0	0	10	0
N2 (% Total)	0	0	10	20	0	20
Fuel Composition						
CH4 (% Fuel)	100	100	100	100	75	75
H2 (% Fuel)	0	0	0	0	25	25
T adiabat. (K)	1754-2232	1790-2024	1790-2107	1790-1967	1802-2033	1663-1977

A variety of diluent and fuel composition conditions were considered as shown in Table 1. The range of equivalence ratios was limited on the lean-side by the occurrence of blow-off. Flame temperatures reported in Table 1 reflect the adiabatic flame temperature, calculated using Cantera and GRI-Mech 3.0 chemistry. Case A consisted of pure methane as a baseline, with cases B through D showing the effects of nitrogen or carbon dioxide dilution. Cases E and F represent test conditions in which both hydrogen addition to the fuel, and nitrogen or carbon dioxide dilution are present. A baseline test case with hydrogen addition is unavailable due to the higher propensity for flashback.

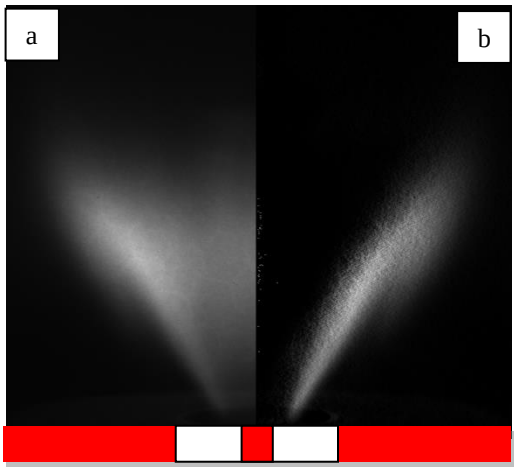

Figure 2 a) Time-averaged image of unstable flame at Q = 150 lpm, f = 0.95, V'rms = 0.3; b) Abel inverted image of the flame surface

RESULTS AND DISCUSSION

The dynamic response of the flame is shown as a function of flame temperature for flows of 125 and 150 lpm in Fig 3a-b. The response for the 100 lpm case was similar although with lower peak amplitudes. While the response varies as a function of flow rate, each plot shows a distinct change in the dynamic response once some threshold temperature is reached. However, unlike the results of Wicksall and Agrawal[14] that displayed a strong dependency of dynamic amplitude on the flame temperature independent of fuel composition, the results shown here suggest that at constant flame temperatures it is possible to modify the dynamic response through the addition of CO2 or N2 in both CH4 and H2/CH4 flames.

It is interesting to note the significant difference in dynamic response observed in flames with 10% CO2 dilution (Fuel B) compared to those with 10% N2 dilution (Fuel C), particularly for Q = 150 lpm. Results plotted in Figure 3b suggest that flames diluted with 20% N2 (Fuel D) had a response more similar to that of the 10% CO2 diluted (Fuel B) case. Of further note, the substitution of 25% H2 in the fuel

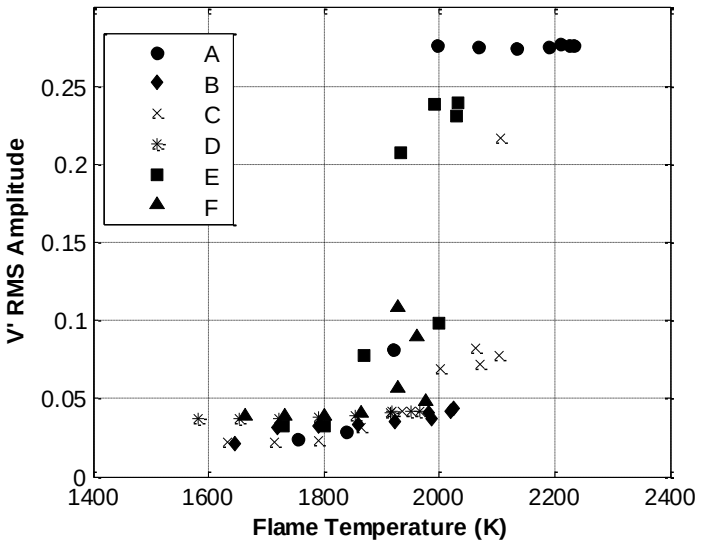

Figure 3. a) Velocity perturbation RMS versus adiabatic flame temperature for Q = 125 lpm.

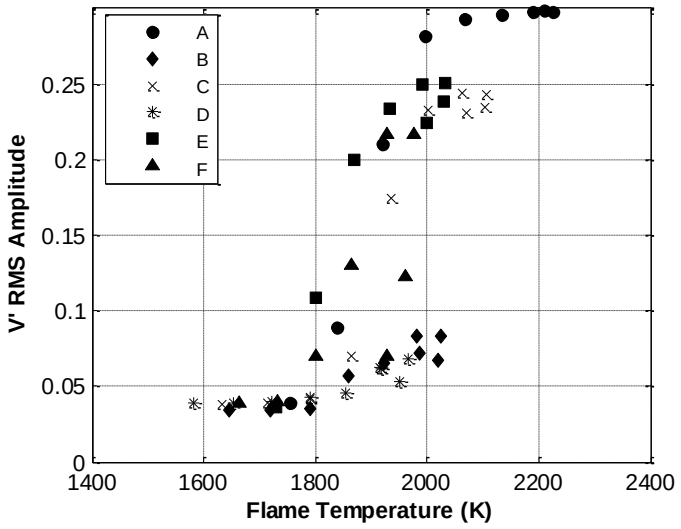

Figure 3. b) Velocity perturbation RMS versus adiabatic flame temperature for Q = 150 lpm.

(Fuel E) did result in an increase of the dynamic response comparable to the 10% N2 diluent (Fuel C) condition.

Lieuwen et al.[9] noted that changes in fuel composition have an impact on the flame speed and subsequently on the flame "center of mass". The center of mass can be defined as the phase averaged center of the CH* intensity (heat release rate) as recorded by the ICCD. The V-shaped flame in question was characterized using the axial and radial distances to the flame center-of-mass, measured from the dump plane and the edge of the center-body, respectively. These measurements may be conveniently reported as a vector quantity, with a magnitude representing the distance from the center-body tip and an angle representing the flame orientation relative to the

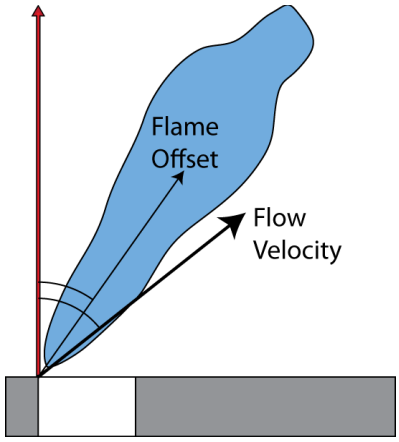

Figure 4. Schematic representation of flame "center of mass" in relation to burner geometry and flow direction.

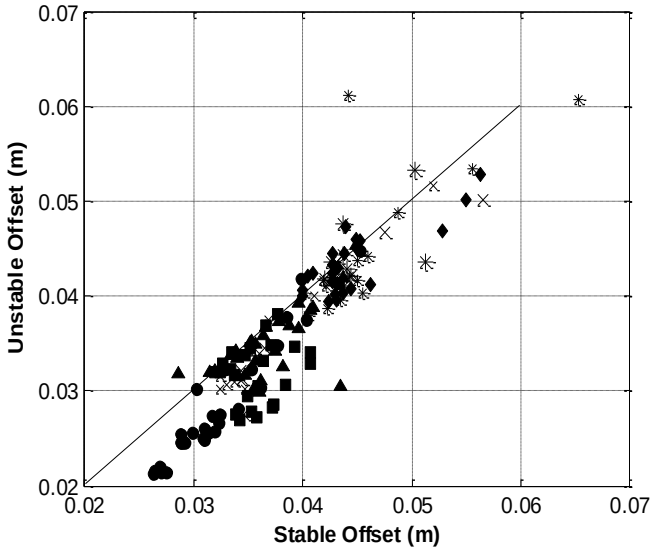

Figure 5. Phase-averaged unstable flame offset versus stable flame offset measured from CH* chemiluminescent images.

vertical. A sketch of this geometry is found in Fig. 4. A plot of the phase averaged unsteady flame center of mass versus the steady flame center of mass is shown in Fig 5 indicating that the measured offset is nearly identical at similar operating conditions suggesting that the unstable flame oscillates around the steady flame location.

The magnitude and angle representing the offset vector for the flame at a flow rate of Q = 125 lpm is found in Figs 6 and 7 respectively. Similar results were obtained at flows of Q = 100 and 150 lpm. The magnitude of the flame offset was observed to decrease with increasing equivalence ratio, reaching a minimum value around an equivalence ratio of Φ=0.95. Adding diluent to the mixture had the effect of elongating the flame. This behavior is intuitive due to the reductions in flame speed expected with dilution. It is interesting to note that the flame offset did not vary significantly even with 50% increases in velocity. This suggests that increases in the velocity are

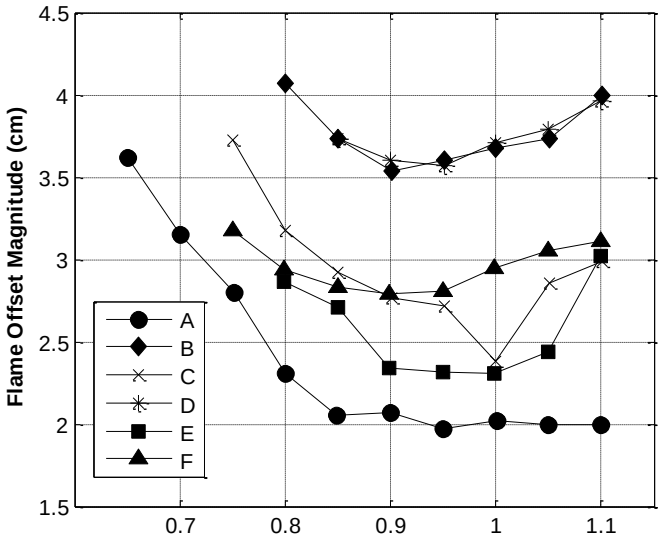

Figure 6. Magnitude of flame offset vector from edge of center body to center of mass, Q = 125 lpm.

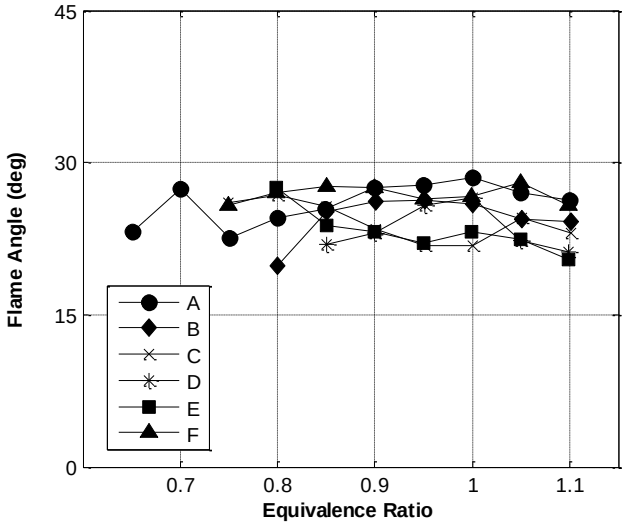

Figure 7. Angle of flame offset vector from vertical, edge of center body to center of mass, Q = 125 lpm

balanced by some other fluid mechanical mechanism which has the effect of reducing the flame size.

Considering the variation of flame angle with respect to operating condition, we may see that there is no obvious trend in the data. The fact that the flame remains approximately at a constant angle for a given composition indicates that the magnitude of the offset primarily results from balanced elongation in both the axial and radial directions.

It is more useful in the context of EGR to understand the changes in flame offset relative to the flame temperature, as shown in Fig. 8. From this figure it is evident that for a flame with the same flame temperature, dilution with either N2 or

CO2 (Cases B, C and D) have longer flames than those without dilution at any given flow rate. Again results from the flame at a flow of Q = 125 lpm are shown while the similar results obtained at Q = 100 and 150 lpm have been removed for clarity. It is of interest to note the difference between fuels B with 10% CO2 diluent and C with 10% N2 diluent. Even for cases of equal calculated flame temperature, the N2 diluted flame has a shorter flame offset. This could be due to a higher specific heat capacity of CO2 at temperature thus allowing CO2 to absorb more heat from the flame subsequently resulting in a longer flame. However, the substitution of 25% of the fuel with H2 (fuel E) produced a shorter flame even with 10% CO2 dilution comparable to that with fuel C. Finally, dilution with 20% N2 (fuels D and F) resulted in flames with similar offset as fuels with 10% CO2 (C and E). These differences are consistent with differences observed in the dynamic response of the burner as shown in Figure 3a and 3b.

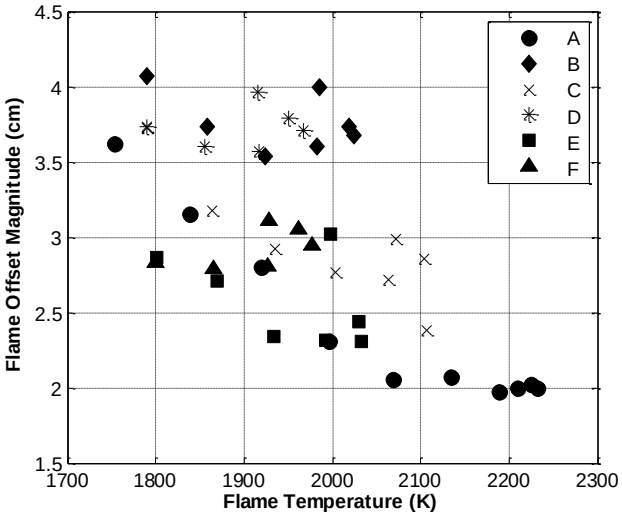

Figure 8. Magnitude of flame offset vector from edge of center body to center of mass versus flame temperature(K), Q = 125 lpm.

The Rayleigh criterion provides boundaries for thermoacoustic instabilities based on the relative phase between the flame heat release rate and acoustic oscillations. It is well known that the flame response to acoustic oscillations is offset in time by a delay associated with convection of disturbances along the flame surface. We may determine this convective delay as a bulk parameter by the distance to the flame center of mass divided by the velocity component along the flame surface. Physically, after an acoustic oscillation interacts with the flame at the flame tip, the disturbance convects along the surface of the flame with the mean flow, resulting in a heat release rate oscillation delayed by the time it takes for this disturbance to reach the flame center of mass. The time delay is compared with the rms value for the velocity oscillations (used as an indicator of unstable amplitude) in Fig. 9 for Q = 125 and 150 lpm (similar results were obtained at Q = 100 lpm although with a lower amplitude). The most significant aspect of this figure is that for the combustor in question, instability did not occur at long time delays (greater than ~6ms). Time delays below 5ms were observed to always be unstable, with time delays greater than 5ms resulting in instabilities of being consistently lower amplitude.

This behavior may be explained by considering the frequencies at which the combustor was observed to oscillate. By plotting the time delay against the unstable frequency for those cases in which instabilities occurred, we see a bifurcation in the region between 5 and 6 ms of time delay, shown in Fig. 10. This region experiences a crossover between two modes of instability, one around 200 Hz and one around 300 Hz. In this case, the adding of diluent allowed this mode to become excited, due to longer time delays associated with the lengthened flames.

We may consider the mode switching effect more closely by observing a contour plot of the velocity oscillation power spectrum. One case with mode switching, composition F with a fuel of 75%CH4/25%H2 and 20% N2 diluent at a flow rate of 125 LPM (triangles in Figure10), is shown in Fig. 11. It is clearly evident from this figure that the mode which exists around 300 Hz is marginally excited for almost the entire equivalence ratio range used. While the lower frequency mode (~210 Hz) dominates at moderate equivalence ratios, continued increases in equivalence ratio shift to the higher frequency mode.

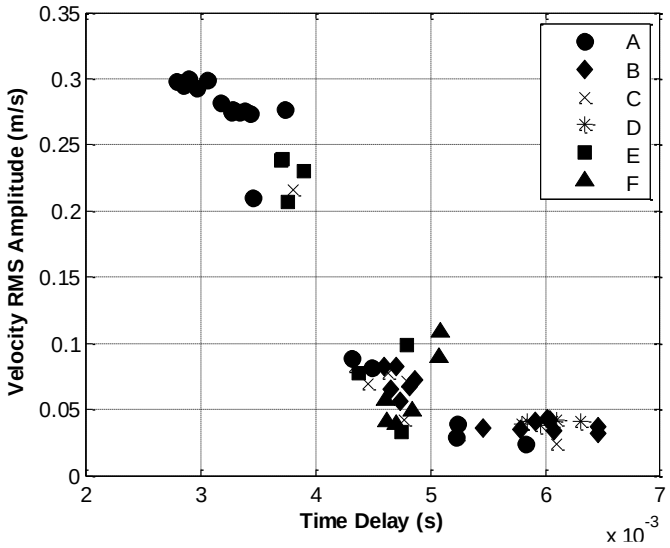

Figure 9. RMS amplitude of velocity perturbations as a function of the convective time delay from the center body type to the flame center of mass, Q = 125 and 150 lpm.

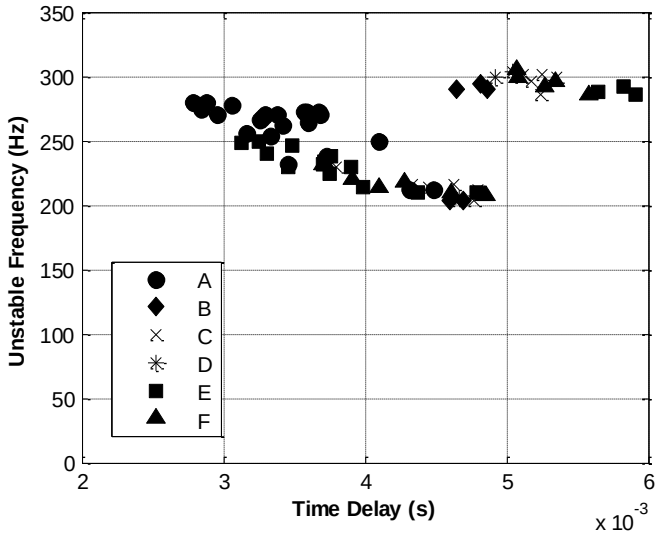

Figure 10. Self-excited frequency as a function of the convective time delay from the center body type to the flame center of mass.

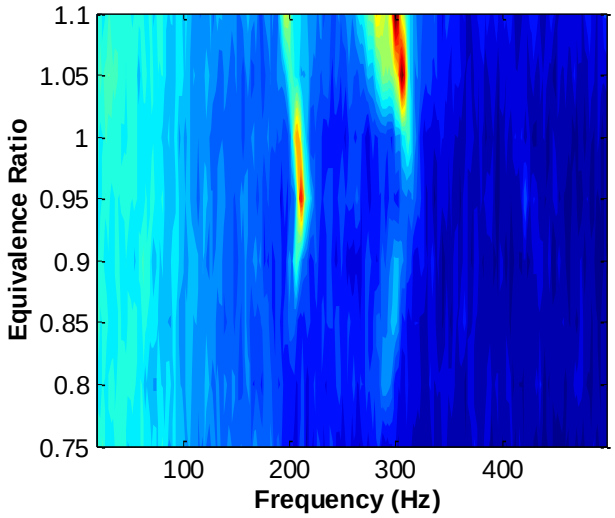

Figure 11. Self-excited frequency as a function of the equivalence ratio showing the effect of mode hopping for Map F (75%CH4/25%H2 – 20%N2) at Q= 125 lpm.

Further investigation of the unstable behavior can be obtained from the non-dimensional frequency in terms of Strouhal number. Strouhal number is defined as the delay time normalized by the period of unstable oscillation[16]. By generating such a plot, we may see that two separate modes of instabilities arise, Fig 12a. The 300 Hz mode in this combustor occurs essentially due to one additional period of delay later than the lower frequency mode. This effect has been described in the literature[9,10] and is similar to the response obtained by

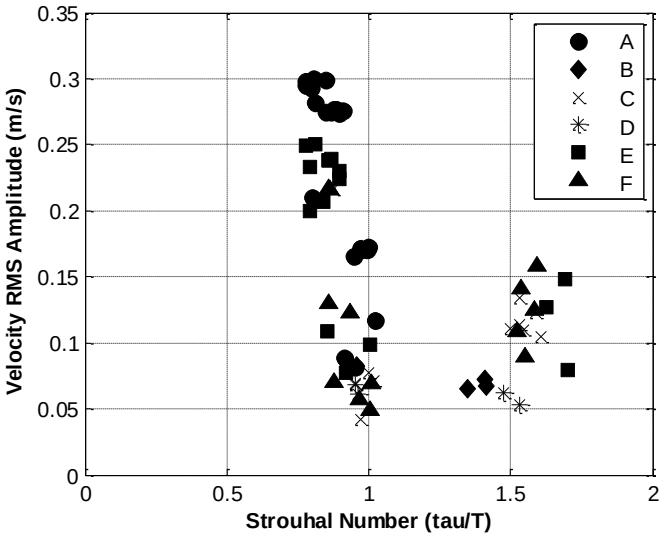

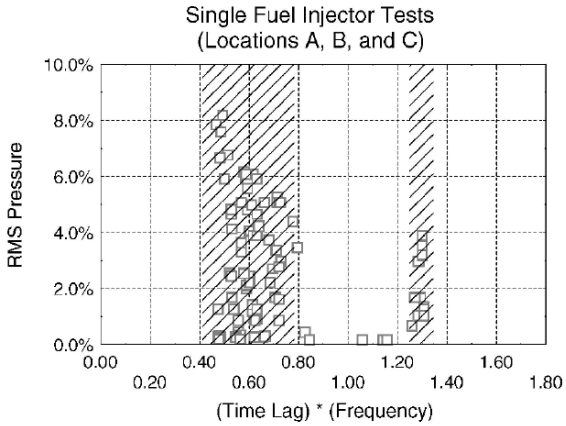

Fig. 15 Data showing experimentally determined stability boundaries for multiple-frequency-mode combustor using the time-lag model.

Figure 12. a) Velocity perturbation amplitude plotted as a function of the non-dimensional time delay, Flame Strouhal Number; b) similar bifurcated response obtained by Richards et al[16].

Richards et al.[16], Fig 12b. This behavior highlights the difficulty of arriving at general statements of the stability behavior of combustion systems. The potential unstable frequencies found in the Strouhal number depend strongly on the system acoustics, making any predictions of instabilities geometry dependent.

The effect of EGR is thus best described through its effect on the time delay. In a practical turbine system, design reasons may lead us to fix the flame temperature. At a fixed flame temperature, EGR cases were observed to result in increased time delay (shown for 125 LPM case in Fig. 13), which for the system in question would be predicted to reduce the occurrence of instabilities.

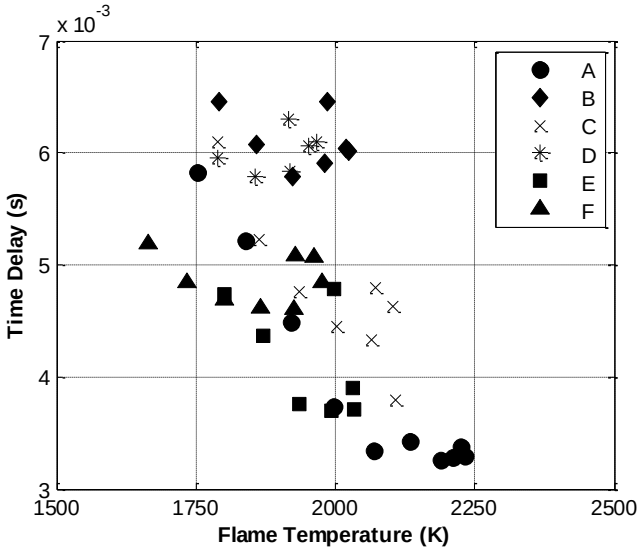

Figure 13. The addition of fuel diluents provide changes in the convective time delays that influence combustion instabilities while maintain a constant flame temperature..

CONCLUSIONS

Proposed strategies for mitigating CO2 emissions from gas turbine based stationary power generation sources could have an impact on fuel composition. This, in turn, could have an undesirable impact on a number of combustion phenomena. In particular, thermoacoustic instabilities are dependent upon convective, chemical and acoustic time scales within the combustor. Changes in fuel composition, through the addition of diluents such as CO2 and N2 can alter the flame location thus changing the phasing of the originating disturbance and subsequent heat release.

Flame location in terms of center-of-mass was found to be unchanged between steady and unsteady flames suggesting that the unsteady flames oscillate around the steady flame location and the average center-of-mass does not change as the flame transitions from a stable to unstable flame. Results from this study supported earlier findings that stressed the importance of convective time delays in unstable systems. In cases with and without diluents, once the time delay reached a limit value the instability amplitude reduced before the instability frequency experienced a bifurcation, or mode hoping, before eventually transitioning to stable operation. This was similar to results show in previous studies.

In both CH4 and CH4/H2 flames the amplitudes of the dynamic instabilities were reduced with the addition of a diluent even while maintaining a constant flame temperature. However, comparable dilution with N2 and CO2 resulted in a difference in the dynamic response as a result of variation in the flame offset. Fuel substitution with 25% hydrogen and 10% CO2 did produce similar results as the 10% N2 dilution with methane. These results suggest that while the addition of dilute may reduce (or more precisely, "change") the dynamic response, varying the amount of CO2 through exhaust gas recirculation could have a larger effect than dilution with air or nitrogen.

ACKNOWLEDGMENTS

This works was supported by the U.S. Department of Energy Turbine Program, Mr. Richard Dennis, Technology Manager.

REFERENCES

1. EPA (2009) "Inventory of U.S. Greenhoususe Gas Emissions and Sinks: 1990 – 2007" *2009 US Greenhouse Gas Inventory Report.* Office of Atmospheric Programs. Available online at: http://www.epa.gov/climatechange/ emissions/downloads09/GHG2007entire_report-508.pdf
2. Energy Information Administration (2009), "International Energy Outlook 2009", Report #:DOE/EIA-0484(2009), Available online at: http://www.eia.doe.gov/oiaf/ieo/ pdf/0484(2009).pdf
3. Botero, C., Finkenrath, M., Bartlett, M., Chu, R., Choi, G., Chinn, D., "Redesign, Optimization and Economic Evaluation of a Natural Gas Combined Cycle with the Best Integrated Technology CO2 Capture", Energy Procedia, 1, pp3835-3842, 2009.
4. Klara, J., "The Potential of Advanced Technologies to Reduce Carbon Capture Costs in Future IGCC Power Plants", Energy Procedia, 1, pp 3827-3834, 2009.
5. Griffin, T., Bücker, D., Pfeffer, A., "Technology Options for Gas Turbine Power Generation with Reduced CO2 Emission", J. Eng. Gas Turbines Power, V 130, July 2008.
6. ElKady, A., Evulet, A., Brand, A., Ursin, T.P., Lynghjem, A., "Exhaust Gas Recirculation in DLN F-Class Gas Turbines for Post-Combustion CO2 Capture", ASME Turbo Expo 2008, GT2008-51152, Berlin, Germany, June 2008.
7. Rokke, P.E., Hustad, J.E., "Exhaust Gas Recirculation in Gas Turbines for Reduction of CO2 Emissions", Intl. J. Thermodynamics, V 8, No. 4, pp 167-173, Sept 2005.
8. Li, H., ElKady, A.M., Evulet, A.T., "Effect of Exhaust Gas Recirculation on NOx Formation in Premixed Combustion System", 47th AIAA Aerospace Sciences, Orlando, Florida, January 2009.
9. Lieuwen, T., McDonell, V., Petersen, E., Santavicca, D., "Fuel Flexibility Influences on Premixed Combustor Blowout, Flashback, Autoignition and Stability", ASME Turbo Expo, GT2006-90770, Barcelona, Spain, June 2006.
10. Lieuwen, T., Zinn, B., "Theoretical Investigation of Combustion Instability Mechanisms in Lean Premixed Gas Turbines", AIAA 98-0641, 36th AIAA Aerospace Sciences Meeting, Reno, Nevada, January 1998.
11. Cong, T.L., Dagaut, P., "Experimental and Detailed Kinetic Modeling of the Oxidation of Methane and Methane / Syngas Mixtures and Effect of Carbon Dioxide

Addition", Combust. Sci and Tech., V180, pp2046-2091, 2008.
12. Noble, D., Zhang, Q., Shareef, A., Tootle, J., Meyeres, A., Lieuwen, T., "Syngas Mixture Composition Effects upon Flashback and Blowout", ASME Turbo Expo, GT2006-90470, 2006.
13. Janus, M., Richards, G., Yip, J., "Effects of Ambinet Conditions and Fuel Composition on Combustion Stability", ASME 97-GT-266, 1997.
14. Wicksall, D.M., Agrawal, A.K., "Acoustics Measurements in a Lean Premixed Combustor Operated on Hydrogen / Hydrocarbon Fuel Mixtures", Intl. J. Hydrogen Energy, V 32, pp1103-1112, 2007.
15. Hendricks, A.G., Vandsburger, U., "The Effect of Fuel Composition on Flame Dynamics", Experimental Thermal and Fluid Science, V 32, No 1, Pages 126-132, October 2007.
16. Richards, G., Straub, D.L., Robey, E.H., "Passive Control of Combustion Dyanmics in Stationary Gas Turbines", J Prop. Power, V19, No5, Sept 2003.
17. Nord, L., Andersen, H.G., "Influence of Variations in the Natural Gas Properties on the Combustion Process in Terms of Emissions and Pulsations for a Heavy-Duty Gas Turbine", IJPGC2003-40188, Atlanta, Georgia, June 2003.
18. Lee, J. G., Santavicca, D. A., *Journal of Propulsion and Power* 19 (5), 735-750, 2003.
19. Samaniego, J. M., Egolfopoulos, F. N., Bowman, C. T. , Combustion Science and Technology 109 (1-6), 183-203, 1995.
20. D. Fritsche, M. Füri, and K. Boulouchos, "An experimental investigation of thermoacoustic instabilities in a premixed swirl-stabilized flame," *Combustion and Flame* 151, no. 1-2 (October 2007): 29-36.
21. Speth, R.L., Altay, H.M., Hudgins, D.E. and Ghoniem, A.F., Dynamics and Stability limits of syngas combustion in a swirl stabilized combustor, 2008 ASME Turbo Expo, June 2008, Berlin, Germany, GT2008-51023.
22. O. Tuncer, S. Acharya, and J.H. Uhm, "Dynamics, NOx and flashback characteristics of confined premixed hydrogen-enriched methane flames," *International Journal of Hydrogen Energy* 34, no. 1 (January 2009): 496-506.